Optics and Laser Technology 124 (2020) 105963

Contents lists available at ScienceDirect

Optics and Laser Technology

journal homepage: www.elsevier.com/locate/optlastec

Measurement of nitric oxide from cigarette burning using TDLAS based on quantum cascade laser

Fei Zheng[a], Xuanbing Qiu[a], Ligang Shao[a], Shiling Feng[a], Tong Cheng[a], Xiaohu He[a], Qiusheng He[a], Chuanliang Li[a,b,*], Ruifeng Kan[b,**], Christa Fittschen[c]

[a] School of Applied Science, Taiyuan University of Science and Technology, Taiyuan 030024, China
[b] State Key Laboratory of Applied Optics, Changchun Institute of Optics, Fine Mechanics and Physics, Chinese Academy of Sciences, Changchun, Jilin 130033, China
[c] Université Lille, CNRS, UMR 8522 - PC2A - Physicochimie des Processus de Combustion et de l'Atmosphère, Lille F-59000, France

HIGHLIGHTS

- A continuous DFB-QCL is first used in TDLAS for measuring emitted NO of cigarette.
- High dynamic response of system is achieved due to a low volume absorption cell.
- An adaptive Kalman filter is employed to reduce the concentration measurement noise.
- Emitted NO masses of cigarette smoke are determined at deferent burning behaviors.

ARTICLE INFO

Keywords:
TDLAS
Cigarette burning
NO
QCL
Kalman filter

ABSTRACT

Nitric oxide (NO) is an important product released by cigarette burning with significantly negative effects to both environment and human health, but it is hard to be measured *in-situ* in the process of burning. In this paper, we report a tunable diode laser absorption spectroscopy (TDLAS) set-up using a quantum cascade laser emitting at 5.24 μm to continuously determine the emitted NO mass in cigarette smoke during burning. Wavelength modulation spectroscopy was applied to improve the detection sensitivity and robustness of the measurement system. A simple single-pass gas cell with a volume of 28 cm^3 was used to record the absorption spectra, and then the mass of NO was derived based on the measured line strength. Allan variance analysis demonstrated that the limit of detection of system reached 28 ppb over 180 s integration time. Due to the low effective volume, the rise time and the fall time were rapid with 3 s and 6 s, respectively. An adaptive Kalman filter was used to reduce the noise on the concentration measurement. As a result, the measurement precision is improved by a factor of 4.5. For accurate determination the total NO mass, the emissions of mainstream (MS) and sidestream (SS) of a burning cigarette were individually measured at the same continuous flow rate. The recorded results of three types of cigarettes revealed that the NO mass emitted in the MS is correlated with the sampling flow rate, while the NO mass emitted by the same cigarette in the SS is hardly influenced by at different smoke flow rates. And different cigarette types with identical physical dimensions emit approximately equivalent mass of NO. This work provides a promising method for determining the mass of emitted NO and other compositions of cigarettes smoke.

1. Introduction

Nitric oxide (NO) is a free radical with an unpaired electron and is the NO_2 precursor, involved in acid deposition and in ozone depletion [1–3]. The presence of NO is universal and its detection and quantification is desired in a variety of fields, such as atmospheric pollutant monitoring [4–6], industrial process gas detection [7,8], and understanding of combustion mechanisms [6,9]. NO, as physiological molecule, can be used as an indicator in disease detection and physiological regulation [10–14]. It is hazardous for human being to be exposed to high NO concentration environments which causes various diseases such as headaches, various diseases, and respiratory distress [1]. NO is

* Corresponding author at: School of Applied Science, Taiyuan University of Science and Technology, Taiyuan 030024, China (C. Li).
** Corresponding author.
E-mail addresses: clli@tyust.edu.cn (C. Li), rfkan@ciomp.ac.cn (R. Kan).

https://doi.org/10.1016/j.optlastec.2019.105963
Received 16 August 2019; Received in revised form 22 October 2019; Accepted 23 November 2019
Available online 10 December 2019
0030-3992/

also a main product of the cigarette smoke. It was reported that the NO concentration could approach 1000 ppm in cigarette smoke [15–17]. Moreover, cigarette combustion is one of the direct pathways for people inhaling high concentrations of NO, so it is necessary to measure the NO released by cigarette burning [16,18].

In recent years, different methods have been applied to analyze NO in cigarette smoke [16,18–24]. Cueto et al. employed a Fourier transform spectrometer with 4 cm^{-1} resolution to measure the variation of NO and nitrogen dioxide (NO_2) concentrations with time, and they investigated the rates of appearance of NO_2 and disappearance of NO of smoke [19]. Shi et al. implemented tunable infrared laser differential absorption spectroscopy to simultaneously measure ammonia, ethylene and NO from mainstream (MS) and sidestream (SS) cigarette smoke. This method was successfully utilized to determine the mass of gases, but an independent carbon dioxide calibration was required to obtain emission ratios [16]. Time-of-flight mass spectrometry with selective photoionization was used to investigate MS smoke by Mitschke et al. [21]. Their instrument could detect a variety of species in smoke and their concentration at puff-by-puff behavior, but the instrument contains a complex vacuum chamber and laser system and thus restricts its wide application due to high cost and bulk. Tunable diode laser absorption spectroscopy (TDLAS) has been widely used to measure gas species due to several advantages, such as high selectivity, high resolution and high sensitivity [25–27]. Therefore, researchers have measured the products of cigarette burning, including NO, by TDLAS [16,28]. However, the previous studies were based on pulsed lead-salt quantum cascade laser (QCL) and bulky volume multi-pass absorption cell. The precision of previous measurements was impeded by the lead-salt laser characteristics of low output power (~ several hundred microwatt) and mode-hop [29]. Moreover, the mirrors of multi-pass absorption cells are vulnerably to be contaminated by particulate matter and tar in the smoke environment. A simple and small volume absorption cell and a high power distributed feedback (DFB)-QCL is used in this work and it is shown that it can improve the conditions for detecting NO in cigarette burning.

Typically, the time scale of noise is very different from fluctuation of the concentration contained in the vapour [30]. The noise of TDLAS originates mainly from optical components, electronic devices and mechanical vibrations. During the measurement of NO in smoke, escaped particulate matter from the cigarette filter can also lead to severe interferences. The Kalman filter is a successful signal post-processing technique [30–32]. It provides an efficient on-line filtering in measurement and can reduce the random noise [33,34]. Therefore, Kalman filter is a suitable solution for improving the measurement of the NO concentration in the harsh environment of cigarette smoke. In this paper, a TDLAS system is reported based on a continuous-wave DFB-QCL and a small single-pass absorption cell. The NO concentration of MS and SS cigarette smoke was derived according to the record intensity of an absorption line from its strong fundamental band around 5.24 μm. Additionally, wavelength modulation spectroscopy (WMS) $-2f$ and the Kalman filter were employed for improving the system's precision and robustness.

2. Experimental

The schematic diagram is shown in Fig. 1. A QCL (Institute of Semiconductors, CAS) operating at 5.24 μm with a linewidth of 0.001 cm^{-1} has been used to scan the absorption doublet R(8.5) line of NO. The output power of the QCL is about 20 mW at 28 °C. The divergence angle of the QCL output mid-infrared beam is less than 10 mrad due to a built-in collimating ZnSe lens. The single-pass absorption cell is made of a quartz tube of 6 mm inner diameter and two CaF_2 windows with Brewster angle, and its length (namely effective optical path length) and volume are 1 m and 28 cm^3, respectively. The laser beam passed through the absorption cell and was focused by a ZnSe lens into an HgCdTe (MCT) detector. A current controller (Wavelength, PLD5K-CH) and a temperature controller (Wavelength, PTC5K-CH) were used to achieve temperature controlling, laser frequency tuning and wavelength modulation. The DAQ card (National Instruments, PCIe-6353) generated a 40 Hz ramp tuning wave and a 40 kHz sinusoidal modulation wave. These signals were superimposed and converted by the digital to analog converter of DAQ. The output analog signal was then transmitted to the laser current controller to implement the wavelength modulation. The signal from the detector was acquired by DAQ card and then demodulated by a LabVIEW program. The gas handling part included a standard NO gas cylinders, nitrogen (N_2) gas cylinders, a pressure controller, a mass flow meter, a vacuum pump, a MS sampling system and a SS sampling system. The NO standard concentration gas and a pure N_2 gas were used to produce the standard NO mixture gases with different concentration levels. A mass flow controller was placed upstream to the absorption cell to adjust the gas flow, while the pressure controller and vacuum pump were placed downstream to the absorption cell in order to control the pressure in the cell. For the MS measurement, the cigarette was held by a supporting holder and the smoke was collected through a sampling orifice. The distance between the sampling orifice and the hot core of the burning cigarette was set to 5 cm for sampling most of the smoke. For the SS measurement, the smoke was collected by a home-made glass cover with a diameter of 15 cm and height of 26 cm. NO is a free radical that reacts easily with O_2. Therefore, prior to the spectroscopic measurement, the cell was purged by pure N_2 to remove O_2 adsorbed on the inner walls of the cell. Besides, a combination of drier (silica gel desiccant breed) and a Cambridge filter (Whatman F319-04) were inserted between the sampling orifice and the absorption cell to decrease water vapor concentration and remove particulate matter.

Three different cigarettes were tested from two typical Chinese commercial cigarette brands: the Lanzhou (LZ) and the regular Huanghelou (HHL) as well as the fine type of Huanghelou (FHHL). Their NO emission was measured by our laser spectrometer. The physical size of the regular type cigarette is 84 mm total length and 7.8 mm diameter, while the fine type cigarette has the same total length as the regular, but has only a diameter of 5.5 mm. The regular LZ and HHL are equivalent with a weight of 900 ± 10 mg while the FHHL weights only half as much. Before each measurement, all the cigarettes were equilibrated to a constant temperature (22 °C) and humidity environment (60%) for 48 h.

3. Results and discussion

3.1. Spectral line selection and measurement

The line of R(8.5) at 1906.73 cm^{-1} from NO's fundamental band was selected to determine the NO concentration in cigarette smoke according to the Beer–Lambert absorption law. At a given pressure, temperature, optical path length, absorption lines and laser parameters (including modulation index) [35,36], the target species concentration (C) is directly proportional to the WMS-2f peak height (P_{2f}) [35].

The R(8.5) transition is a discrete line without overlapping of absorption lines of other main products contained in the cigarette smoke, thus avoiding interferences from other species of the burning cigarette. The optimal signal was obtained at a total pressure of 90 Torr in the absorption cell and a modulation amplitude of 2.5 mV derived by a series of measurements. The corresponding modulation depth is 2.2 [25]. A series of standard concentrations of NO in the range of 18 to 720 ppm were measured by WMS-2f. The demodulating frequency was set at 2 * 40 kHz for achievement of WMS-2f. For experimental calibration, NO from three different standard cylinders containing 1000 ppm, 600 ppm and 100 ppm were diluted with N_2. A serial of known NO concentrations diluted by N_2 were recorded for 40 s, as shown in Fig. 2(a). The linear relationship between WMS-2f amplitudes and concentrations is presented in Fig. 2(b). The linear relationship is:

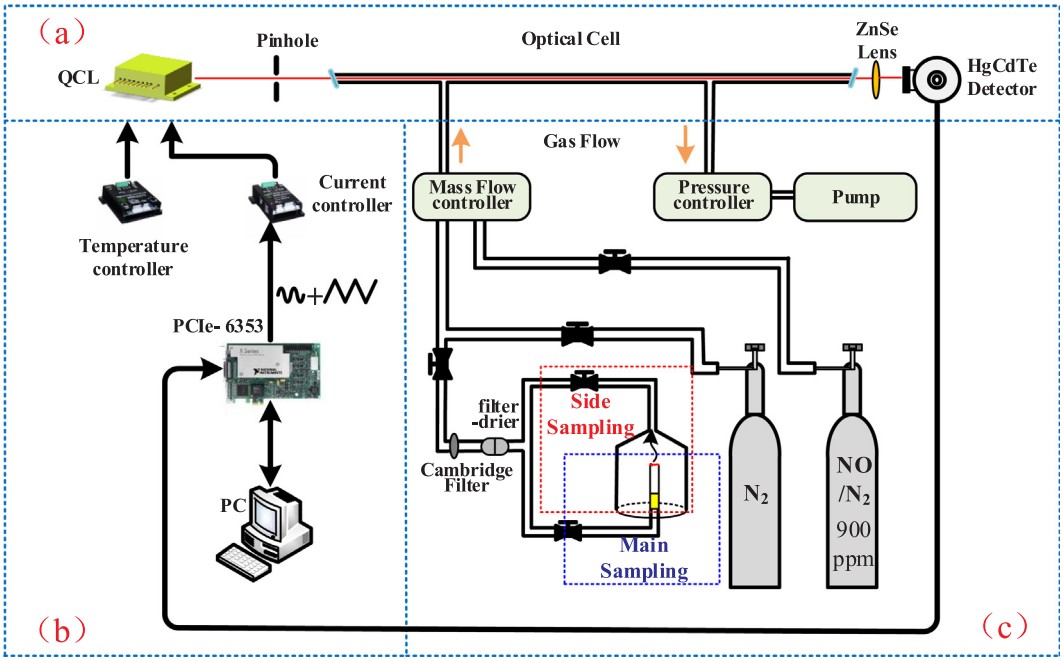

Fig. 1. Schematic diagram of experimental setup for detecting NO emitted from burning cigarette. Fig. 1(a) shows optical path, Fig. 1(b) shows electrical part and Fig. 1(c) is gas handling system.

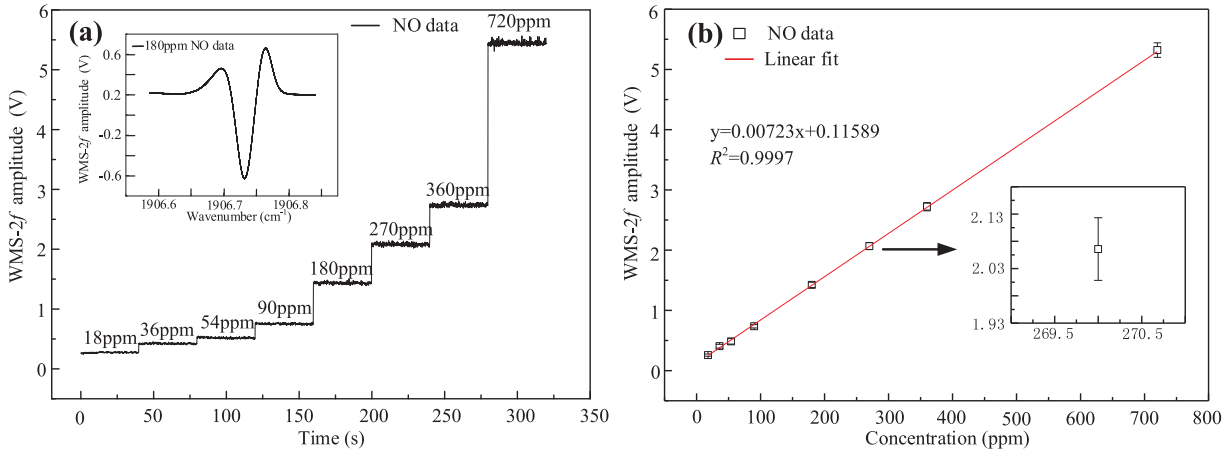

Fig. 2. (a) Measured NO WMS-2f signal amplitude in the range of 18–720 ppm and WMS-2f signal of 180 ppm; (b) The linear relationship between observed signal and NO concentration.

$$C = 0.00723 * P_{2f} + 0.11589 \quad (1)$$

This equation is used to determine the concentration of *in-situ* NO in cigarette burning. The value of correlation coefficients (R^2) is 0.9997 and the standard deviation of the fitted value is 0.02016, indicating the high quality of fitting.

The stability and limit of detection(LOD) of the system were analyzed by Allan variance. The unprocessed raw data are plotted in Fig. 3(a), and the Allan variance as a function of the measurement time is depicted in Fig. 3(b). It implies that the optimum integration time is 180 s and the LOD is 28 ppb. The histogram corresponding to the NO concentration distribution histogram is shown in Fig. 3(c), and it obviously resembles a Gaussian distribution. Thus, a Gaussian function has been employed to fit the distribution and the fitting profile is also plotted in Fig. 3(c). As a result, the R^2 value, the half-width at half-maximum and the standard deviation value (σ) were calculated to be 0.98, 2.85 ppm and 1.32 ppm, respectively. The results demonstrate the excellent stability and precision of the NO measuring system. The dynamic response test of the system has been performed at the flow rate of 500 mL/min and the result shown in Fig. 4. The entrance port of the sampling cell was connected through a "Y"-type line with a cylinder containing 600 ppm NO and another one containing pure N_2. The two cylinders could be switched "on" or "off" by two solenoid valves for the test of response time. The entrance port was also connected to a pressure controller. The rise time (10–90%) and the fall time (90–10%) approach 3 s and 6 s, respectively, demonstrating the benefit of the low volume of the absorption cell.

3.2. Signal processing

An adaptive Kalman filter was applied to improve the detection sensitivity and precision of the measurements [35]. In the Kalman filter recursive procedure, the current estimation ($\widehat{X}_k$) is predicted from previous estimation ($\widehat{X}_{k-1}$), the equation is:

$$\widehat{X}_k = \widehat{K}_k \cdot \widehat{Z}_k + (1 - \widehat{K}_k) \cdot \widehat{X}_{k-1} \quad (2)$$

where $\widehat{Z}_k$ is the measurement value and the $\widehat{K}_k$ is Kalman gain. The values of σ_ω^2 is the true concentration variability and σ_ν^2 is the

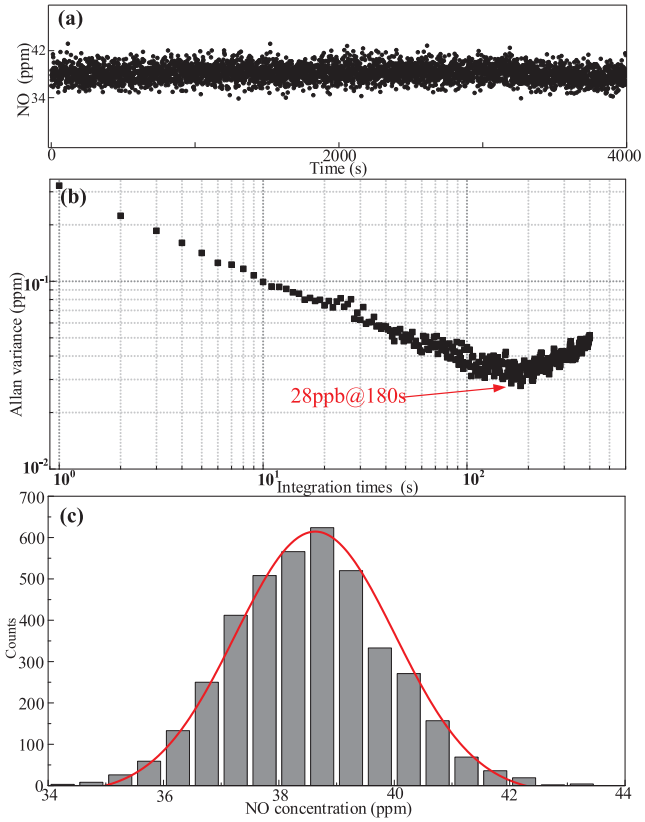

Fig. 3. (a) The unprocessed raw data (b) Allan variance as a function of integration time; (c) Histogram of NO concentrations distribution.

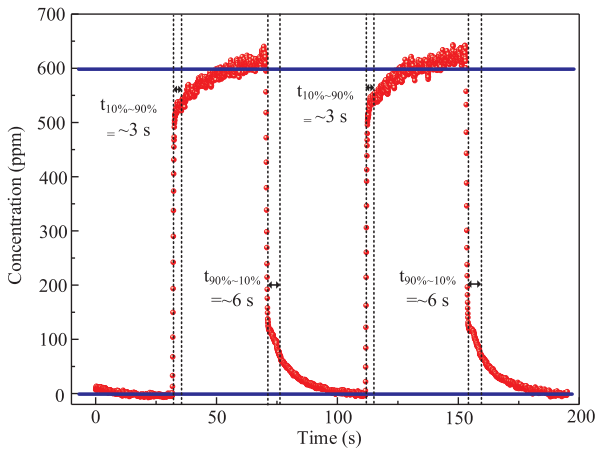

Fig. 4. Response time test by varying the NO concentration between 0 and 600 ppm.

measurement noise introduced by the instrument. The ratio of $\sigma_v^2/\sigma_\omega^2$ (ϱ) is a constant and is a key parameter in tuning the Kalman filter. It is susceptible when ϱ is set to a small value, while the filtering lag appears at large ϱ value [32,33,37]. A series of empirical values was tried for obtaining the optimum ϱ value, and the best results were derived at ϱ equal to 80.

A comparison between low-pass Infinite Impulse Response (IIR) filter and Kalman filter was carried out to prove the advantage of Kalman filtering, as illustrated in Fig. 5. The black line shows the raw data for the concentration of NO from the HHL cigarette, the blue and the red lines represent the low-pass IIR Butterworth and the Kalman filterings, respectively. Both filtering methods can reduce the noise of raw data, but Kalman filter possesses a higher efficiency. As plotted in

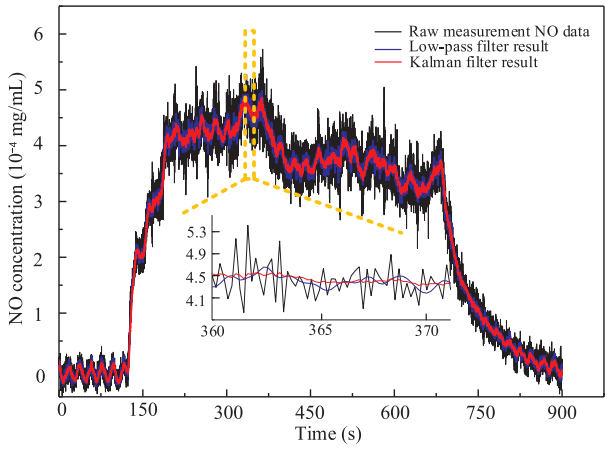

Fig. 5. The raw concentration of NO (black line) of the HHL cigarette. The low-pass filter (blue line) and a Kalman filter (red line) were used to improve the detection precision. (For interpretation of the references to colour in this figure legend, the reader is referred to the web version of this article.)

the insert of Fig. 5, the Kalman filter shows superiority to the low-pass filter in rapid response and precision. The standard deviation of the raw data was $3.6 * 10^{-5}$ mg/mL. The standard deviations of the low-pass and Kalman filtered signal were $1.2 * 10^{-5}$ mg/mL and $0.79 * 10^{-5}$ mg/mL, respectively. Thus, the detection precision was improved by a factor of 4.5 by Kalman filter, which is better than the performance of the low-pass filter.

3.3. Determination of the mass of NO emission of burning cigarettes

We can obtain the mass of NO emission using the following equation:

$$m = \int_0^V C * \rho dv = \int_0^V C * MPT_0/P_0 TV_m dv \quad (3)$$

where C is the concentration, ρ is the density, M is the molar mass of the NO, P and T are pressure and temperature in the laboratory, respectively, and V_m is the molar volume of the gas under standard conditions, taken as 22.4 L/ mol. When the NO was sampled from the MS, the valves of SS and N_2 were closed. The cigarette was kept burning and the smoke continuously entered the optical absorption cell through the sampling orifice. The NO concentration was determined from the recorded spectral line intensity based on Beer–Lambert absorption law.

For investigating the mechanism producing the NO of burning cigarettes, four different flow rates of smoke sampling were employed. As shown in Fig. 6(a), the NO concentration in MS of the same type of cigarette varies with the sampling flow rates. The higher the flow rate was set the lower the observed NO concentration was. Our results are reasonable because the NO formation is significantly relevant with the burning temperature [8]. It is prone to formation of NO at a high temperature combustion environment [38]. More combustion heat is transferred by high sampling flow rate, so the combustion temperature of the cigarette at high flow rate is lower than at low flow rates. For a fixed flow rate, more O_2 will pass through the core when the cigarette burns short, so the full combustion obtained results in a higher reaction temperature. Therefore, the maximum NO concentration for each flow rate is observed at the end of the burning, as plotted in Fig. 6(a). NO from SS was sampled by a glass cover, and the cigarette was kept smoldering during the measurement. The recorded NO concentrations of the same type of cigarette are presented in Fig. 6(b). As a result of air dilution, the NO concentration in the sampling cell decreases with the increase of the sampling flow rate and the dilution factor needs to be taken into account for calculating the total emitted NO mass. As a result, the total emitted NO mass is nearly equal at different flow rate, as listed Table 1.

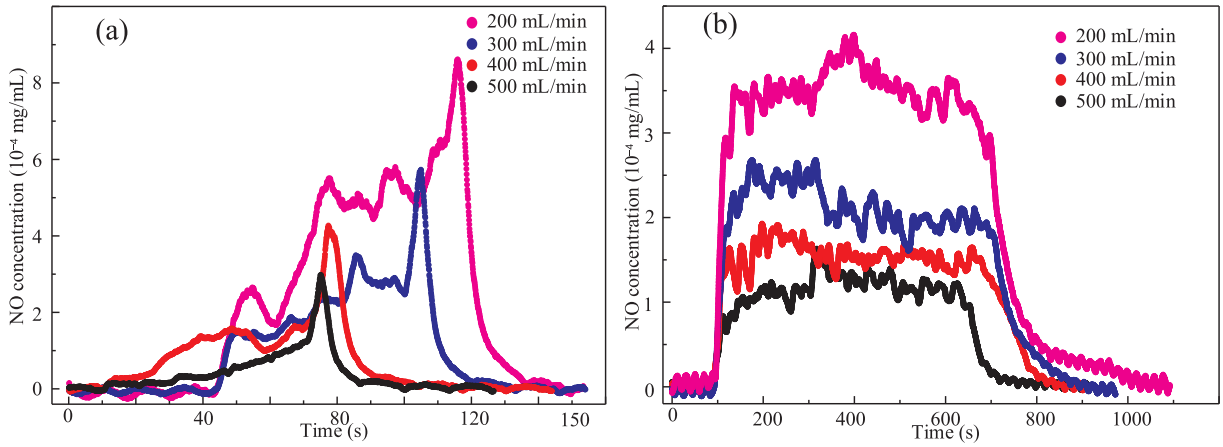

Fig. 6. (a) The NO concentration of LZ' MS smoke at different flow rates; (b) The NO concentration of LZ' SS smoke at different flow rates.

Table 1
The emitted NO mass (milligram per cigarette) in the MS and SS smoke for different cigarettes and the uncertainty of measured value after symbol is standard deviation from 5 times measurements.

	MS			SS		
Flow (mL/min)	LZ	HHL	FHHL	LZ	HHL	FHHL
200	0.180 ± 0.014	0.19 ± 0.05	0.170 ± 0.006	0.750 ± 0.004	0.760 ± 0.007	0.64 ± 0.09
300	0.12 ± 0.05	0.16 ± 0.02	0.120 ± 0.013	0.72 ± 0.09	0.75 ± 0.01	0.63 ± 0.08
400	0.11 ± 0.01	0.08 ± 0.01	0.070 ± 0.015	0.72 ± 0.09	0.74 ± 0.04	0.61 ± 0.09
500	0.070 ± 0.005	0.057 ± 0.003	0.040 ± 0.023	0.67 ± 0.03	0.67 ± 0.08	0.60 ± 0.08

The total emitted NO mass of each cigarette type was derived and tabulated in Table 1. The variation trends of the total emitted NO mass at different flow rates are similar for different types of cigarette. The emitted NO mass per cigarette is essentially equivalent for both regular cigarettes LZ and HHL for both MS and SS. Interestingly, it is only slightly higher for the regular compared to the fine one. In Randall et al.'s measurement [20], the total emitted NO mass of SS smoke from Kentucky Reference cigarette 2R4F, IMI7 and IMI6 were 1.7 ± 0.2 mg, 1.3 ± 0.2 mg and 1.5 ± 0.2 mg, respectively, the corresponding emitted NO mass of MS smoke were 0.24 ± 0.05 mg, 0.28 ± 0.05 mg and 0.35 ± 0.06 mg, respectively. Shi et al. measured the total emitted NO mass per cigarette of Kentucky Reference cigarette 1R4F and 1M16 [16]. They reported the emitted NO mass from MS of Kentucky Reference cigarette 1R4F and 1M16 being 0.28 ± 0.05 mg and 0.38 ± 0.06 mg, and the ones of SS smoke were 1.8 ± 0.3 mg and 1.7 ± 0.3 mg. In comparisons, our results are only about one third of these previous measurements. The difference can be caused by the sampling method, of which we detected the NO mass of cigarettes at continuous burning and smoldering states, while Randall et al. and Shi et al. measured simultaneously with intra-puff profiles for mainstream and with continuous measurement of sidestream smoke [16,20]. Besides, the physical parameters of different types of cigarettes, such as weight, physical size and origin of the tobacco, can differ from the previous ones and might explain the different results.

4. Conclusion

A QCL TDLAS set-up coupled to a small volume absorption cell has been used to measure the emitted NO mass in cigarette smoke. The WMS-2*f* technique together with the Kalman filter method was applied to improve the accuracy and the robustness of the system. The LOD reached 28 ppb over 180 s integration time, and the rise and fall time were rapid with 3 s and 6 s, respectively. The emitted NO mass of three types of cigarettes were measured at different flow rates. Our results of both MS and SS are in reasonable agreement with previous studies. The paper shows that the current set-up is a promising method for determining the emitted NO mass and other products (such as CO, NH_3 and HCN) of burning cigarettes.

Declaration of Competing Interest

The authors declare that they have no known competing financial interests or personal relationships that could have appeared to influence the work reported in this paper.

Acknowledgement

This work was supported by the National Natural Science Foundation of China (Grant Nos. U1810129, U1610117 and 11904252), State Key Laboratory of Applied Optics (SKLAO-201902), Excellent Youth Academic Leader in Higher Education of Shanxi Province (2018), Key Research and Development Program of Shanxi Province of China (Grant Nos. 201803D31077 and 201803D121090), the Fund for Shanxi "1331 Project" Key Innovative Research Team (1331KIRT), Natural Science Foundation of Shanxi Province of China (No. 201801D221017) and the Fund for Shanxi Key Subjects Construction.

Appendix A. Supplementary material

Supplementary data associated with this article can be found, in the online version, at https://doi.org/10.1016/j.optlastec.2019.105963.

References

[1] H.S. Kim, K.U. Jang, T.W. Kim, NOx gas detection characteristics in FET-type multi-walled carbon nanotube-based gas sensors for various electrode spacings, J. Korean Phys. Soc. 68 (2016) 797–802, https://doi.org/10.3938/jkps.68.797.
[2] T. Francis, Bioluminescent assay for nitric oxide utilizing the biological enzyme activity of soluble guanylate cyclase, Anal. Lett. 44 (2011) 2834–2840, https://doi.org/10.1080/00032719.2011.565446.
[3] H. Wu, X. Yin, L. Dong, Z. Jia, J. Zhang, F. Liu, W. Ma, L. Zhang, W. Yin, L. Xiao,

et al., Ppb-level nitric oxide photoacoustic sensor based on a mid-IR quantum cascade laser operating at 52°C, Sensors Actuat. B: Chem. 290 (2019) 426–433, https://doi.org/10.1016/j.snb.2019.04.007.
[4] D. Nelson, J. Shorter, J. McManus, M. Zahniser, Sub-part-per-billion detection of nitric oxide in air using a thermoelectrically cooled mid-infrared quantum cascade laser spectrometer, Appl. Phys. B 75 (2002) 343–350, https://doi.org/10.1007/s00340-005-2058-0.
[5] R. Lewicki, J.H. Doty, R.F. Curl, F.K. Tittel, G. Wysocki, Ultrasensitive detection of nitric oxide at 5.33 μm by using external cavity quantum cascade laser-based Faraday rotation spectroscopy, Proc. Nat. Acad. Sci. 106 (2009) 12587–12592, https://doi.org/10.1073/pnas.0906291106.
[6] X. Chao, J.B. Jeffries, R.K. Hanson, In situ absorption sensor for NO in combustion gases with a 5.2 μm quantum-cascade laser, Proc. Combust. Inst. 33 (2011) 725–733, https://doi.org/10.1016/j.proci.2010.05.014.
[7] Y. Yamamoto, H. Sumizawa, H. Yamada, K. Tonokura, Real-time measurement of nitrogen dioxide in vehicle exhaust gas by mid-infrared cavity ring-down spectroscopy, Appl. Phys. B 105 (2011) 923–931, https://doi.org/10.1007/s00340-011-4647-4.
[8] Z. Wang, X. Liu, Y. Mu, X. Yang, Z. Jiang, et al., The exhaust emission online detection on the diesel engine, Optik 164 (2018) 126–131, https://doi.org/10.1016/j.ijleo.2018.02.047.
[9] X. Chao, J. Jeffries, R. Hanson, Wavelength-modulation-spectroscopy for real-time, in situ NO detection in combustion gases with a 5.2 μm quantum-cascade laser, Appl. Phys. B 106 (2012) 987–997, https://doi.org/10.1007/s00340-011-4839-y.
[10] M. Bernareggi, G. Cremona, Measurement of exhaled nitric oxide in humans and animals, Pulmonary Pharmacol. Therapeut. 12 (1999) 331–352, https://doi.org/10.1006/pupt.1999.0216.
[11] C. Roller, K. Namjou, J. Jeffers, W. Potter, P. McCann, J. Grego, Simultaneous NO and CO_2 measurement in human breath with a single IV–VI mid-infrared laser, Opt. Lett. 27 (2002) 107–109, https://doi.org/10.1364/OL.27.000107.
[12] C. Roller, K. Namjou, J.D. Jeffers, M. Camp, A. Mock, P.J. McCann, J. Grego, Nitric oxide breath testing by tunable-diode laser absorption spectroscopy: application in monitoring respiratory inflammation, Appl. Opt. 41 (2002) 6018–6029, https://doi.org/10.1364/AO.41.006018.
[13] S. Cristescu, D. Marchenko, J. Mandon, K. Hebelstrup, G. Griffith, L. Mur, F. Harren, Spectroscopic monitoring of NO traces in plants and human breath: applications and perspectives, Appl. Phys. B 110 (2013) 203–211, https://doi.org/10.1007/s00340-012-5050-5.
[14] Y.A. Bakhirkin, A.A. Kosterev, C. Roller, R.F. Curl, F.K. Tittel, Mid-infrared quantum cascade laser based off-axis integrated cavity output spectroscopy for biogenic nitric oxide detection, Appl. Opt. 43 (2004) 2257–2266, https://doi.org/10.1364/AO.43.002257.
[15] K. Alving, C. Fornhem, E. Weitzberg, J. Lundberg, Nitric oxide mediates cigarette smoke-induced vasodilatory responses in the lung, Acta Physiol. Scandinavica 146 (1992) 407–408, https://doi.org/10.1111/j.1748-1716.1992.tb09439.x.
[16] Q. Shi, D.D. Nelson, J.B. McManus, M.S. Zahniser, M.E. Parrish, R.E. Baren, K.H. Shafer, C.N. Harward, Quantum cascade infrared laser spectroscopy for real-time cigarette smoke analysis, Anal. Chem. 75 (2003) 5180–5190, https://doi.org/10.1021/ac034217y.
[17] R.R. Baker, Smoke generation inside a burning cigarette: modifying combustion to develop cigarettes that may be less hazardous to health, Progress Energy Combust. Sci. 32 (2006) 373–385, https://doi.org/10.1016/j.pecs.2006.01.001.
[18] T. Adam, S. Mitschke, T. Streibel, R.R. Baker, R. Zimmermann, Quantitative puff-by-puff-resolved characterization of selected toxic compounds in cigarette mainstream smoke, Chem. Res. Toxicol. 19 (2006) 511–520, https://doi.org/10.1021/tx050220w.
[19] R. Cueto, D.R. Church, W.A. Piyor, Quantitative fourier transform infrared analysis of gas phase cigarette smoke and other gas mixtures, Anal. Lett. 22 (1989) 751–763, https://doi.org/10.1080/00032718908051362.
[20] R.E. Baren, M.E. Parrish, K.H. Shafer, C.N. Harward, Q. Shi, D.D. Nelson, J.B. McManus, M.S. Zahniser, Quad quantum cascade laser spectrometer with dual gas cells for the simultaneous analysis of mainstream and sidestream cigarette smoke, Spectrochim. Acta Part A: Mol. Biomol. Spectrosc. 60 (2004) 3437–3447, https://doi.org/10.1016/j.saa.2003.11.048.
[21] S. Mitschke, T. Adam, T. Streibel, R.R. Baker, R. Zimmermann, Application of time-of-flight mass spectrometry with laser-based photoionization methods for time-resolved on-line analysis of mainstream cigarette smoke, Anal. Chem. 77 (2005) 2288–2296, https://doi.org/10.1021/ac050075r.
[22] B.T. Thompson, B. Mizaikoff, Real-time fourier transform-infrared analysis of carbon monoxide and nitric oxide in sidestream cigarette smoke, Appl. Spectrosc. 60 (2006) 272–278, https://doi.org/10.1366/000370206776342616.
[23] Z. Bacsik, J. McGregor, J. Mink, FTIR analysis of gaseous compounds in the mainstream smoke of regular and light cigarettes, Food Chem. Toxicol. 45 (2007) 266–271, https://doi.org/10.1016/j.fct.2006.08.018.
[24] D. Moir, W.S. Rickert, G. Levasseur, Y. Larose, R. Maertens, P. White, S. Desjardins, A comparison of mainstream and sidestream marijuana and tobacco cigarette smoke produced under two machine smoking conditions, Chem. Res. Toxicol. 21 (2007) 494–502, https://doi.org/10.1021/tx050220w.
[25] X. Guo, F. Zheng, C. Li, X. Yang, N. Li, S. Liu, J. Wei, X. Qiu, Q. He, A portable sensor for in-situ measurement of ammonia based on near-infrared laser absorption spectroscopy, Opt. Lasers Eng. 115 (2019) 243–248, https://doi.org/10.1016/j.optlaseng.2018.12.005.
[26] C. Li, L. Shao, H. Meng, J. Wei, X. Qiu, Q. He, W. Ma, L. Deng, Y. Chen, High-speed multi-pass tunable diode laser absorption spectrometer based on frequency-modulation spectroscopy, Opt. Exp. 26 (2018) 29330–29339, https://doi.org/10.1364/OE.26.029330.
[27] C. Li, Y. Wu, X. Qiu, J. Wei, L. Deng, Pressure-dependent detection of carbon monoxide employing wavelength modulation spectroscopy using a herriott-type cell, Appl. Spectrosc. 71 (2017) 809–816, https://doi.org/10.1177/0003702816682194.
[28] J.H. Shorter, D.D. Nelson, M.S. Zahniser, M.E. Parrish, D.R. Crawford, D.L. Gee, Measurement of nitrogen dioxide in cigarette smoke using quantum cascade tunable infrared laser differential absorption spectroscopy (TILDAS), Spectrochim. Acta Part A: Mol. Biomol. Spectrosc. 63 (2006) 994–1001, https://doi.org/10.1016/j.saa.2005.11.005.
[29] J. Shemshad, S.M. Aminossadati, M.S. Kizil, A review of developments in near infrared methane detection based on tunable diode laser, Sensors Actuat. B: Chem. 171 (2012) 77–92, https://doi.org/10.1016/j.snb.2012.06.018.
[30] H. Riris, C.B. Carlisle, R.E. Warren, Kalman filtering of tunable diode laser spectrometer absorbance measurements, Appl. Opt. 33 (2017) 5506–5508, https://doi.org/10.1364/AO.33.005506.
[31] R.E. Kalman, A new approach to linear filtering and prediction problems, Trans. ASME, J. Basic Eng. 82 (1960) 35–45, https://doi.org/10.1115/1.3662552.
[32] B. Fang, W. Zhao, X. Xu, J. Zhou, X. Ma, S. Wang, W. Zhang, D.S. Venables, W. Chen, Portable broadband cavity-enhanced spectrometer utilizing kalman filtering: application to real-time, in situ monitoring of glyoxal and nitrogen dioxide, Opt. Exp. 25 (2017) 26910–26922, https://doi.org/10.1364/OE.25.026910.
[33] D. Leleux, R. Claps, W. Chen, F. Tittel, T. Harman, Applications of kalman filtering to real-time trace gas concentration measurements, Appl. Phys. B 74 (2002) 85–93, https://doi.org/10.1007/s0034001007513.
[34] J. Chen, A. Hangauer, R. Strzoda, M.C. Amann, Laser spectroscopic oxygen sensor using diffuse reflector based optical cell and advanced signal processing, Appl. Phys. B 100 (2010) 417–425, https://doi.org/10.1007/s00340-010-3956-3.
[35] G. Wang, J. Mei, X. Tian, K. Liu, T. Tan, W. Chen, X. Gao, Laser frequency locking and intensity normalization in wavelength modulation spectroscopy for sensitive gas sensing, Opt. Exp. 27 (2019) 4878–4885, https://doi.org/10.1364/OE.27.004878.
[36] J. Liu, J. Jeffries, R. Hanson, Wavelength modulation absorption spectroscopy with 2f detection using multiplexed diode lasers for rapid temperature measurements in gaseous flows, Appl. Phys. B 78 (2004) 503–511, https://doi.org/10.1364/OE.27.004878.
[37] Y. Meng, T. Liu, K. Liu, J. Jiang, R. Wang, T. Wang, H. Hu, A modified empirical mode decomposition algorithm in TDLAS for gas detection, IEEE Photonics J. 6 (2014) 1–7, https://doi.org/10.1109/JPHOT.2014.2368785.
[38] A. Frassoldati, T. Faravelli, E. Ranzi, Kinetic modeling of the interactions between no and hydrocarbons at high temperature, Combust. Flame 135 (2003) 97–112, https://doi.org/10.1016/S0010-2180(03)00152-4.